

Leading correction to the local density approximation for exchange in large- Z atoms

Nathan Argaman

*Department of Physics, Nuclear Research Center—Negev,
P.O. Box 9001, Be'er Sheva 84190, Israel; argaman@mailaps.org*

Jeremy Redd

Department of Physics, Utah Valley University, Orem, UT 84058, USA

Antonio C. Cancio

Department of Physics and Astronomy, Ball State University, Muncie, IN 47306, USA

Kieron Burke

*Departments of Physics and Astronomy and of Chemistry,
University of California, Irvine, CA 92697, USA*

(Dated: 4 October, 2022)

The large- Z asymptotic expansion of atomic energies has been useful in determining exact conditions for corrections to the local density approximation in density functional theory. The correction for exchange is fit well with a leading $Z\ln Z$ term, and we find its coefficient numerically. The gradient expansion approximation also has such a term, but with a smaller coefficient. Analytic results in the limit of vanishing interaction with hydrogenic orbitals (a Bohr atom) lead to the conjecture that the coefficients are precisely 2.7 times larger than their gradient expansion counterparts, yielding an analytic expression for the exchange-energy correction which is accurate to $\sim 5\%$ for all Z .

For almost a century, the non-relativistic semiclassical expansion of the total binding energy of atoms [1] has guided the development of density functional approximations, beginning with Thomas-Fermi (TF) theory [2, 3] and the local density approximation (LDA) for exchange [4, 5]. In the seventies, Lieb and Simon proved [6] that the dominant term in that expansion is given exactly by TF theory, and in the eighties Schwinger and Englert showed explicitly that the LDA recovers the dominant term for the atomic exchange energy [7–9]. Recent analytic and numerical evidence shows the same is true for atomic correlation energies [10, 11].

For exchange, recent focus has been on the leading correction to LDA [12, 13], see Fig. 1. Most modern generalized gradient approximations (GGAs) — the starting point of most modern exchange–correlation approximations — yield a well-defined correction that can be compared to atomic data for large Z . The popular approximations known as PBE [14] and B88 [15] both yield highly accurate approximations to this term for atoms, which are about double that of the gradient-expansion approximation [16, 17] (GEA), yielding some of the insight behind PBEsol [18]. The behavior for large Z has been built into several recent non-empirical approximations (SCAN [19], APBE [20], acGGA [11]).

The original works [12, 13] on expanding the beyond-LDA exchange energy for atoms,

$$\Delta E_x = E_x - E_x^{\text{LDA}}, \quad (1)$$

used simple powers of $Z^{1/3}$, based on the scaling behavior of the gradient expansion for the slowly-varying electron gas. Here we provide three lines of evidence for the existence of a $Z\ln Z$ contribution, showing that the analytic forms used as ‘exact conditions’ are likely incorrect, and should be

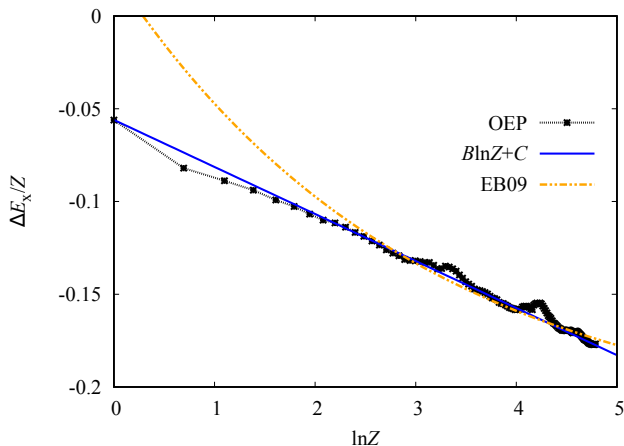


FIG. 1. Beyond-LDA exchange energy per electron ($\Delta E_x/Z$) of neutral atoms. The solid blue line is the new $B\ln Z + C$ fit described in the text, whereas the orange dashed curve is the fit of Ref. [13]. (Hartree atomic units used throughout.)

replaced by those suggested below. Thus, the current work not only contributes to the very long-standing search for the expansion of the energy of atoms in mathematical physics, but also provides a crucial correction to exact conditions which are built into the latest modern density functional approximations, used throughout condensed matter physics, materials science, and chemistry.

Our first line of inquiry consists of evaluating $\Delta E_x/Z$ for neutral atoms up to $Z = 120$, using the optimized effective potential (OEP). These data are plotted versus $\ln Z$ in Fig. 1, and a straight line gives a significantly better fit than Ref. [13].

A second direction shows analytically that applying the GEA to the TF density profile for an atom [21] produces a $\ln Z$ divergence near the nucleus, but its coefficient is less than half the slope of the fit in Fig. 1, reflecting the aforementioned discrepancy with GGAs.

A third direction is a study of the Bohr atom [22], in which the electron repulsion is infinitesimal and the orbitals are hydrogenic. Exchange energies were calculated analytically for such atoms with up to 22 closed shells [23]. Fitting these, as well as the LDA exchange energies, gives a $Z\ln Z$ coefficient larger than that of neutral, interacting-electron atoms. In GEA, the cusp where the Bohr-atom TF density abruptly vanishes also contributes. Overall, the $Z\ln Z$ coefficient is here 2.7 times larger than in GEA. Assuming that ratio is true for all atoms explains the data of Fig. 1.

Our first step is a detailed analysis of Fig. 1. Three candidates for the leading correction to LDA are: a term proportional to Z [13], the $Z\ln Z$ dependence suggested by the GEA, and a term proportional to $Z^{4/3}$, which appears in the oscillations across the periodic table [24]. The general form

$$\Delta E_x/Z \approx -A' Z^{1/3} - B\ln Z - C - DZ^{-1/3} \quad (2)$$

enables a discussion of all these possibilities.

We use the OPMKS code [25] to calculate E_x with the OEP and E_x^{LDA} with the spin-dependent LDA of [26], for non-relativistic neutral atoms up to $Z = 120$, extending an earlier data set [10]. To avoid bias, we ignore the large numbers of highly correlated data points across subshells, keeping only atoms with closed subshells, grouped as follows: He and the alkaline earths (s), the remaining noble gases (p), group 12 metals (d), and closed f-shell atoms. There are 20 such atoms for $Z \leq 120$, but we exclude the first element of each group ($Z = 2, 10, 30$, and 70), as these are most strongly affected by oscillations in Z [10].

To generate a set of competing models for our data, we vary a subset of coefficients in Eq. (2), holding the others to zero, and find the coefficients and their standard errors from nonlinear regression using the Levenberg-Marquardt method [27]. These are shown in Table I, listed in order of the number of parameters, with data entries for zeroed out coefficients left blank. The final column shows the reduced χ^2 of the fit, i.e., the sum of the squared errors per degree of freedom, $\chi_{\text{red}}^2 = \sum_{i=1}^n (\frac{\delta_i}{\sigma})^2 / (n - m)$. Here δ_i is the difference between the two sides of Eq. (2) for the i th value of Z , the standard error σ has been set to 1 mHa for simplicity, and m is the number of free parameters in the fit.

For the first (and worst) two forms, $\Delta E_x \propto Z$ is the leading order, as in Ref. [13]. The logarithmic fit, line 3, has the smallest errors in coefficients and the best χ_{red} . This fit does remarkably well also *outside* the range of Z fitted, even down to hydrogen, as seen in Fig. 1.

The remaining fits have additional free parameters. A $Z^{1/3}$ term (fits 5 and 7) slightly degrades the quality of the fit, in the sense that χ_{red} increases ($n - m$ decreases more than $\sum_i \delta_i^2$), and the standard error of the A' coefficient

	A'	B	C	D	χ_{red}^2
1			0.153(6)		560
2			0.2138(34)	-0.205(11)	22.1
3		0.02464(26)	0.0590(10)		0.91
4		0.0256(14)	0.053(9)	0.008(12)	0.95
5	0.0007(15)	0.0239(16)	0.0592(11)		0.96
6	0.0128(9)		0.134(5)	-0.098(7)	1.3
7	-0.007(8)	0.039(16)	0.01(5)	0.06(7)	0.98

TABLE I. Coefficients of various fits of $\Delta E_x/Z$ in Eq. (2), with “missing” coefficients fixed at zero. χ_{red}^2 quantifies the errors of the fit as described in the text. Standard errors in the coefficients are given in parenthesis.

is larger than its absolute value, suggesting it should be set to zero [13]. A term proportional to $Z^{-1/3}$ is likewise ineffective (fits 4 and 7). Fit 6, using only powers of $Z^{1/3}$ without a logarithmic term, results in a somewhat larger $\sum_i \delta_i^2$ despite the larger number of free parameters.

An asymptotic series should increase in accuracy as Z increases, so we refit models to a more restricted set of data: first by dropping a second element of each group (12 atoms), and then a third (9 atoms). For the $\ln Z$ -leading model, the three fits yield essentially the same results ($B = 0.0254, 0.0253$ and $C = 0.0560, 0.0562$). For the $Z^{1/3}$ model (fit 6), the coefficients drift noticeably as the data is restricted to a smaller range, and the fit is poor outside the range fitted, similar to the EB09 curve in Fig. 1. As a final test, using all data from $Z = 1$ to 120 indiscriminately yields coefficients for B and C that are statistically indistinguishable from those of fit 3, but with a much higher χ_{red}^2 . The data and details of the fits are given in [28].

Overall, the fits with the $\ln Z$ term as leading order are clearly the most predictive, and for best judgement of the asymptotic behavior we choose the 12-atom fit of the $\ln Z$ model, which is appropriately weighted to large Z (the 9-atom fit gives larger standard errors for B and C [28]):

$$\Delta E_x \approx -0.0254Z\ln Z - 0.0560Z, \quad (3)$$

which is the curve shown in Fig. 1. Remarkably, given that E_x^{LDA} is -0.2564 for hydrogen, this yields -0.3124 , almost exactly matching the analytic result, $-5/16$. That the success of this fit should in fact be expected of the semiclassical approximation is evident in Figs. 1 and 9 of [10] and in [29]. Before such an asymptotic expansion diverges, the inclusion of the next term will often improve accuracy by two orders of magnitude [29, 30]. Eq. (3) thus provides another example of “the principle of unreasonable utility of asymptotic estimates” [31].

Next, we estimate ΔE_x theoretically. The LDA exchange energy is given by

$$E_x^{\text{LDA}} = -a_x \int d^3r n^{4/3}(\mathbf{r}), \quad (4)$$

where $a_x = 3(3/\pi)^{1/3}/4$ [4, 5], and insertion of the TF density [21] into this expression directly gives the dominant

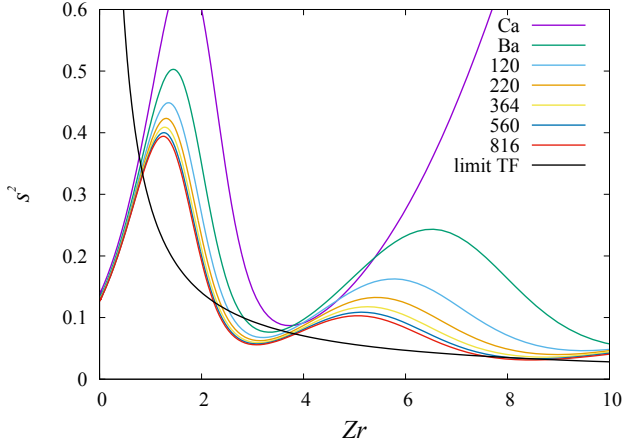


FIG. 2. Plot of s^2 near the nucleus versus distance, scaled as Zr , for alkaline earth atoms ranging from Ca up to $Z = 816$ which has valence shell $16s^2$. The black line shows the TF model.

contribution [10] to exchange as $Z \rightarrow \infty$, $E^{\text{TF}} = -AZ^{5/3}$. For the beyond-LDA contribution to the exchange energy, Eq. (1), we try the GEA [17, 32],

$$\Delta E_x^{\text{GEA}} = -\mu^{\text{GE}} a_x \int n^{4/3}(\mathbf{r}) s^2(\mathbf{r}) d^3r, \quad (5)$$

where $s = |\nabla n|/(2k_F n)$ is the dimensionless gradient parameter, $k_F = (3\pi^2)^{1/3} n^{1/3}$ is the local Fermi wavenumber, and $\mu^{\text{GE}} = 10/81$ [33]. Application of Eq. (5) to the slowly-varying gas, or to a neutral atom using the density scaling of [12], yields a term of order Z when scaled toward the TF limit. However, the present analysis amounts to scaling the potential, in the sense of Refs. [34, 35]. While potential- and density-scaling are interchangeable for the dominant term of the large- Z asymptotic expansion (TF theory), additional terms appear for potential scaling, such as the Scott correction to the kinetic energy [21]. To show this for exchange, we proceed by directly employing the TF profile in Eq. (5).

Gradients are weak in the bulk of large atoms, with s of order $Z^{-1/3}$. At distances smaller than $O(Z^{-1/3})$ from the nucleus, screening of the nuclear charge is negligible [22] and the TF density varies as $(2Z/r)^{3/2}/3\pi^2$, so

$$s^{\text{TF}}(r) \simeq \frac{3}{4} \frac{1}{\sqrt{2Z}r}, \quad r \ll Z^{-1/3}. \quad (6)$$

This approximation fails in the region where the inner shell (1s) electrons dominate; see Fig. 2, which shows s^2 of alkaline earths up to $Z = 816$ (using FHI98PP in all-electron mode [36]) and s^2 of the TF density, Eq. (6). For $r \gg 1/Z$, the atomic gradients approach the TF curve, while near $r \approx 1/Z$, the density profile displays the oscillations studied in [22] and switches over to that of the well-known nuclear cusp, while s remains finite, achieving its maximum value around $r = 1/Z$. Keeping only the

divergent contribution to Eq. (5) gives:

$$\Delta E_x^{\text{GEA}} \simeq -\frac{9\mu^{\text{GE}}}{8\pi^2} Z \int_{Z^{-1}}^{Z^{-1/3}} \frac{dr}{r}, \quad (7)$$

which yields a logarithmic term,

$$\Delta E_x^{\text{GEA}} = -\frac{3\mu^{\text{GE}}}{4\pi^2} Z \ln Z + O(Z). \quad (8)$$

We define

$$B = -\lim_{Z \rightarrow \infty} \Delta E_x / (Z \ln Z), \quad (9)$$

and our derivation yields

$$B^{\text{GEA}} = \frac{3}{4\pi^2} \mu^{\text{GE}} \quad (10)$$

or about 9.38 mHa. The presence of such a logarithmic term in the GEA for atoms was noticed in [37], and could be inferred from earlier work (see Appendix A of [11]).

We have no rationale for the difference between the result of the GEA, Eq. (10), and the actual data, Eq. (3), i.e., the slope in Fig. 1. The GEA result is unaffected by integration by parts (unlike [38]). Thus, the beyond-LDA exchange energy of large- Z atoms has a leading $Z \ln Z$ term both numerically and in GEA, but their coefficients disagree.

A similar analysis can be applied to the analog of Eq. (5) for the kinetic energy, leading to a stronger divergence at small r , due to the presence of an extra power of $n^{1/3}$. In addition to the naive-scaling $Z^{5/3}$ term, the small- r cutoff produces a Z^2 term, proportional to the Scott correction mentioned above. This procedure does not generate the exact coefficient, $-1/2$ (see [21]). Instead this is inferred from the Bohr atom [10], to which we turn for the analysis of exchange.

The simplicity of the Bohr atom (hydrogenic orbitals) allows calculations to much larger electron number, leading to unambiguous results. We fill N hydrogenic orbitals in a potential $-N/r$, so that N plays the role of Z here. The inner region, $r \ll N^{-1/3}$, is identical to that of interacting atoms in the large Z limit [39].

We analytically evaluated E_x , defined by an infinitesimal Coulomb repulsion, up to $N = 7590$ (22 shells), using Mathematica [23]. Our extremely accurate fit has the form

$$E_x^{\text{Bohr}}(N) = -\bar{A}_o N^{5/3} - (\bar{B}_o \ln N + \bar{C}_o) N - (\bar{D}_o \ln N + \bar{E}_o) N^{1/3} + \dots, \quad (11)$$

where the subscript denotes a Bohr-atom coefficient and the bar denotes E_x . The leading coefficient is $(2/3)^{1/3}(4/\pi^2)$, from LDA applied to the TF density [39], while $\bar{B}_o = 26.268$ mHa agrees with $7/(27\pi^2)$ to 5 digits, with $\bar{C}_o = 45.3536$ mHa, $\bar{D}_o = -3.17$ mHa and $\bar{E}_o = 0.6$ mHa, determined to the number of digits shown (see [28] for details).

For LDA, there are also $O(N^{2/3} \ln N)$ and $O(N^{2/3})$ terms, making results harder to fit. However, the simplicity of the expressions [22] and availability of arbitrary precision software (using the Julia language with 64-decimal-digit

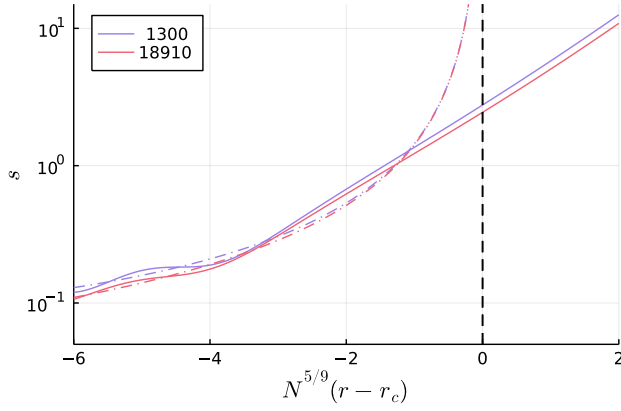


FIG. 3. Plot of the gradient parameter s near the edge of the Bohr atom, versus distance from the cusp radius r_c , scaled by $N^{5/9}$, for two representative values of N identified in the legend. Dot-dashed lines: the results of the corresponding TF models, which diverge at r_c (dashed vertical line).

accuracy) enables their brute-force evaluation for up to 100 full shells ($N = 676700$) [28]. We find B_o^{LDA} to match $-2/(27\pi^2)$ to within $\sim 0.1\%$ (note the opposite sign), yielding

$$B_o = \bar{B}_o - B_o^{\text{LDA}} = \frac{1}{3\pi^2}. \quad (12)$$

To evaluate the GEA, note the TF density distribution:

$$n_o^{\text{TF}} = \frac{(2N)^{3/2}}{3\pi^2} (r^{-1} - r_c^{-1})^{3/2}, \quad r \leq r_c, \quad (13)$$

where $r_c = (18/N)^{1/3}$ is the radius beyond which the density vanishes [39], so s diverges not only at the nucleus but also as r approaches r_c [39], as

$$s_o^{\text{TF}} \simeq \frac{3}{4} \frac{3^{2/3}}{2^{1/6}} \left[N^{5/9} (r_c - r) \right]^{-3/2}, \quad 0 < r_c - r \ll N^{-1/3}. \quad (14)$$

The result is

$$\Delta E_o^{\text{GEA}} \simeq -\frac{9\mu^{\text{GE}}}{8\pi^2} N \left[\int_{N^{-1}}^{N^{-1/3}} \frac{dr}{r} + \int_0^{r_c - N^{-5/9}} \frac{dr}{r_c - r} \right], \quad (15)$$

where the first logarithmic divergence is treated as above. The second is also cut off, taking into account that the kinetic energy is here very small, and the wavelength of the electrons is of order $N^{-5/9}$ [40], as displayed in Fig. 3. As a result, the contribution of the second divergence is 3 times smaller than that of the first, yielding

$$B_o^{\text{GEA}} = \frac{\mu^{\text{GE}}}{\pi^2}. \quad (16)$$

The two regions of divergence also determine B_o^{LDA} . The inner region of the density has been studied in detail in [22]. The leading non-oscillatory correction to the TF density

profile is $n(r) \simeq n^{\text{TF}}(r)[1 - 1/(64Zr)]$ for $Z^{-1} \ll r \ll Z^{-1/3}$, producing a contribution of $-1/(18\pi^2)$ via Eq. (4). Consistency with the result $B_o^{\text{LDA}} = -2/(27\pi^2)$, Eq. (12), requires that the outer divergence yields a contribution $1/3$ as large as the first, just as for B_o^{GEA} .

The value excogitated from the highly precise numerical results, Eq. (12), is exactly $27/10$ times larger than that of the GEA, Eq. (16). It is tempting to conjecture that

$$B = \frac{27}{10} B^{\text{GEA}} \quad (17)$$

yields the exact result for *all* atoms, including fully interacting ones, implying that $B = 1/(4\pi^2)$ or 25.3 mHa is the exact result for neutral atoms, in agreement with our fit, Eq. (3). More generally, the conjecture gives the prediction

$$B = \frac{1}{12\pi^2} \left(4 - \frac{N}{Z} \right) \quad (18)$$

for any N/Z ratio, interpolating between the result for neutral atoms, $N = Z$, and Eq. (12) for $N \ll Z$. A careful investigation of this relationship will require generating data for a large range of N for each N/Z ratio, as in Fig. 1. As a preliminary check, we show in [28] that applying this formula with a constant C to a number of positive ions with $N/Z = 1/2$ continues to give agreement with the beyond-LDA data from the OEP, at the $\sim 5\%$ level, for $N > 2$.

Last, we turn to the implications for approximate functional development. Our derivation applies to most GGA's for the exchange energy, usually written in terms of an enhancement factor F_x :

$$E_x^{\text{GGA}} = -a_x \int n^{4/3}(\mathbf{r}) F_x(s(\mathbf{r})) d^3r. \quad (19)$$

Typically, $F_x \approx 1 + \mu^{\text{GGA}} s^2 + \dots$ for small s , which dominates in the TF limit. Thus Eq. (10) applies, with μ^{GE} replaced by μ^{GGA} . This yields 16.7 mHa for PBE and 20.9 mHa for B88, differing from the value of 25.4 mHa of Eq. (3). However, both yield accurate E_x for Z between 10 and 100, due to differences in the remaining terms of a large- Z fit. Thus, functionals that have been fit to large- Z data, such as SCAN, are accurate for all practical calculations. In the future both the $O(Z \ln Z)$ and the $O(Z)$ terms should be addressed in developing approximate density functionals.

Using the hydrogen atom as a 'norm' [19], the conjecture above yields:

$$\Delta E_x^{\text{normed}} = -Z \left\{ \frac{\ln Z}{4\pi^2} + \frac{5}{16} - 0.2564 \right\} \quad (20)$$

for neutral atoms, which is indistinguishable from the straight line of Fig 1, and contains no empirical parameters.

In conclusion, the present work is a step in the process of improving density functional approximations using asymptotic expansions for non-relativistic atoms: it identifies a logarithmic divergence in the coefficient of the leading $O(Z)$ contribution to the beyond-LDA exchange energy, resulting in a leading $Z \ln Z$ term.

Further steps would involve studying existing approximations, evaluating the coefficients of both their $Z\ln Z$ terms and their $O(Z)$ terms. Obtaining very-high- Z data for real atoms is crucial, possibly using simplified methods. Analogous data for molecules and solids would also be very helpful, especially to determine any differences based on the lack of classical turning surfaces in solids [41]. But first and foremost, a derivation of the $Z\ln Z$ term from semiclassical theory, including the correct value

of its coefficient, would provide a fundamental, detailed understanding of the exchange energy, and would be instrumental in guiding future developments in density functional theory.

This research was supported by the NSF (CHE-2154371). We thank Paola Gori-Giorgi for communicating a preprint of [37] and for the ensuing valuable discussions, and John Snyder for unpublished notes.

-
- [1] B.-G. Englert, *Semiclassical theory of atoms*, Lec. Notes Phys., Vol. 300 (Springer, 1988).
- [2] L. H. Thomas, "The calculation of atomic fields," *Math. Proc. Camb. Phil. Soc.* **23**, 542–548 (1927).
- [3] E. Fermi, "Eine statistische methode zur bestimmung einiger eigenschaften des atoms und ihre anwendung auf die theorie des periodischen systems der elemente (A statistical method for the determination of some atomic properties and the application of this method to the theory of the periodic system of elements)," *Zeitschrift für Physik* **48**, 73–79 (1928).
- [4] F. Bloch, "Bemerkung zur elektronentheorie des ferromagnetismus und der elektrischen leitfähigkeit (Remark on the electron theory of ferromagnetism and electrical conductivity)," *Zeitschrift für Physik* **57**, 545–555 (1929).
- [5] P. A. M. Dirac, "Note on exchange phenomena in the Thomas atom," *Mathematical Proceedings of the Cambridge Philosophical Society* **26**, 376–385 (1930).
- [6] Elliott H Lieb and Barry Simon, "The Thomas-Fermi theory of atoms, molecules and solids," *Advances in Mathematics* **23**, 22 – 116 (1977).
- [7] Julian Schwinger, "Thomas-Fermi model: The second correction," *Phys. Rev. A* **24**, 2353–2361 (1981).
- [8] Berthold-Georg Englert and Julian Schwinger, "Thomas-Fermi revisited: The outer regions of the atom," *Phys. Rev. A* **26**, 2322–2329 (1982).
- [9] B.-G. Englert and J. Schwinger, "Semiclassical atom," *Phys. Rev. A* **32**, 26 (1985).
- [10] Kieron Burke, Antonio Cancio, Tim Gould, and Stefano Pittalis, "Locality of correlation in density functional theory," *The Journal of Chemical Physics* **145**, 054112 (2016).
- [11] Antonio Cancio, Guo P. Chen, Brandon T. Krull, and Kieron Burke, "Fitting a round peg into a round hole: asymptotically correcting the generalized gradient approximation for correlation," *The Journal of Chemical Physics* **149**, 084116 (2018).
- [12] John P. Perdew, Lucian A. Constantin, Espen Sagvolden, and Kieron Burke, "Relevance of the slowly varying electron gas to atoms, molecules, and solids," *Phys. Rev. Lett.* **97**, 223002 (2006).
- [13] Peter Elliott and Kieron Burke, "Non-empirical derivation of the parameter in the b88 exchange functional," *Can. J. Chem.* **87**, 1485–1491 (2009).
- [14] John P. Perdew, Kieron Burke, and Matthias Ernzerhof, "Generalized gradient approximation made simple," *Phys. Rev. Lett.* **77**, 3865–3868 (1996), *ibid.* **78**, 1396(E) (1997).
- [15] A. D. Becke, "Density-functional exchange-energy approximation with correct asymptotic behavior," *Phys. Rev. A* **38**, 3098–3100 (1988).
- [16] D.A. Kirzhnits, "Quantum corrections to the Thomas-Fermi equation," *Sov. Phys. JETP* **5**, 64 (1957).
- [17] R. M. Dreizler and E. K. U. Gross, *Density Functional Theory: An Approach to the Quantum Many-Body Problem* (Springer-Verlag, Berlin, 1990).
- [18] John P. Perdew, Adrienn Ruzsinszky, Gábor I. Csonka, Oleg A. Vydrov, Gustavo E. Scuseria, Lucian A. Constantin, Xiaolan Zhou, and Kieron Burke, "Restoring the density-gradient expansion for exchange in solids and surfaces," *Phys. Rev. Lett.* **100**, 136406 (2008).
- [19] Jianwei Sun, Adrienn Ruzsinszky, and John P. Perdew, "Strongly constrained and appropriately normed semilocal density functional," *Phys. Rev. Lett.* **115**, 036402 (2015).
- [20] Lucian A. Constantin, E. Fabiano, S. Laricchia, and F. Della Sala, "Semiclassical neutral atom as a reference system in density functional theory," *Phys. Rev. Lett.* **106**, 186406 (2011).
- [21] Donghyung Lee, Lucian A. Constantin, John P. Perdew, and Kieron Burke, "Condition on the kohn–sham kinetic energy and modern parametrization of the thomas–fermi density," *J. Chem. Phys.* **130**, 034107 (2009).
- [22] Ole J. Heilmann and Elliott H. Lieb, "Electron density near the nucleus of a large atom," *Phys. Rev. A* **52**, 3628–3643 (1995).
- [23] J. C. Snyder, J. Ovadia, D. Lee, K. Ray, and K. Burke, "Using hydrogenic orbitals to improve density functional theory," American Chemical Society Meeting Abstract 71-COMP (2011).
- [24] B.-G. Englert and J. Schwinger, "Atomic-binding-energy oscillations," *Phys. Rev. A* **32**, 47 (1985).
- [25] E. Engel and R. M. Dreizler, "From explicit to implicit density functionals," *Journal of Computational Chemistry* **20**, 31–50 (1999).
- [26] John P. Perdew and Yue Wang, "Accurate and simple analytic representation of the electron-gas correlation energy," *Phys. Rev. B* **45**, 13244–13249 (1992).
- [27] William H. Press, Saul A. Teukolsky, William T. Vetterling, and Brian P. Flannery, eds., *Numerical Recipes*, 3rd ed. (Cambridge University Press, New York, 2007).
- [28] See Supplemental Material at <http://link.aps.org/supplemental/10.1103/PhysRevLett.129.153001> (or at dft.uci.edu) for the numerical values of the exchange energies and details of the fits.
- [29] M V Berry and Kieron Burke, "Exact and approximate energy sums in potential wells," *Journal of Physics A: Mathematical and Theoretical* **53**, 095203 (2020).
- [30] Kieron Burke, "Leading correction to the local density approximation of the kinetic energy in one dimension," *The Journal of Chemical Physics* **152**, 081102 (2020),

<https://doi.org/10.1063/5.0002287>.

- [31] J. Schwinger, "Thomas-Fermi model: The leading correction," *Phys. Rev. A* **22**, 1827 (1980).
- [32] P. Hohenberg and W. Kohn, "Inhomogeneous electron gas," *Phys. Rev.* **136**, B864–B871 (1964).
- [33] L. Kleinman and S. Lee, "Gradient expansion of the exchange-energy density functional: Effect of taking limits in the wrong order," *Phys. Rev. B* **37**, 4634 (1988).
- [34] Attila Cangi, Donghyung Lee, Peter Elliott, Kieron Burke, and E. K. U. Gross, "Electronic structure via potential functional approximations," *Phys. Rev. Lett.* **106**, 236404 (2011).
- [35] Attila Cangi, E. K. U. Gross, and Kieron Burke, "Potential functionals versus density functionals," *Phys. Rev. A* **88**, 062505 (2013).
- [36] Martin Fuchs and Matthias Scheffler, "Ab initio pseudopotentials for electronic structure calculations of poly-atomic systems using density-functional theory," *Computer Physics Communications* **119**, 67–98 (1999).
- [37] Timothy J. Daas, Derk P. Kooi, Arthur J. A. F. Grooteman, Michael Seidl, and Paola Gori-Giorgi, "Gradient expansions for the large-coupling strength limit of the Møller–Plesset adiabatic connection," *Journal of Chemical Theory and Computation* **18**, 1584–1594 (2022), <https://doi.org/10.1021/acs.jctc.1c01206>.
- [38] J.P. Perdew, V. Sahni, M.K. Harbola, and R.K. Pathak, "Fourth-order gradient expansion of the fermion kinetic energy: Extra terms for non-analytic densities," *Phys. Rev. B* **34**, 686 (1986).
- [39] Aaron D. Kaplan, Biswajit Santra, Puskar Bhattarai, Kamal Wagle, Shah Tanvir ur Rahman Chowdhury, Pradeep Bhetwal, Jie Yu, Hong Tang, Kieron Burke, Mel Levy, and John P. Perdew, "Simple hydrogenic estimates for the exchange and correlation energies of atoms and atomic ions, with implications for density functional theory," *The Journal of Chemical Physics* **153**, 074114 (2020), <https://doi.org/10.1063/5.0017805>.
- [40] W. Kohn and A. E. Mattsson, "Edge electron gas," *Phys. Rev. Lett.* **81**, 3487 (1998).
- [41] Aaron D. Kaplan, Stewart J. Clark, Kieron Burke, and John P. Perdew, "Calculation and interpretation of classical turning surfaces in solids," *npj Computational Materials* **7**, 2057–3960 (2021).

Supplementary Material for “Leading correction to the local density approximation for exchange in large- Z atoms”

Nathan Argaman

*Department of Physics, Nuclear Research Center—Negev,
P.O. Box 9001, Be’er Sheva 84190, Israel; argaman@mailaps.org*

Jeremy Redd

Department of Physics, Utah Valley University, Orem, UT 84058, USA

Antonio C. Cancio

Department of Physics and Astronomy, Ball State University, Muncie, IN 47306, USA

Kieron Burke

*Departments of Physics and Astronomy and of Chemistry,
University of California, Irvine, CA 92697, USA*

(Dated: 4 October, 2022)

Tables of exchange-energy data for neutral atoms, positive ions and Bohr atoms are given, as well as details of the fits to asymptotic expansions in the number of electrons.

1. ENERGIES FOR NEUTRAL ATOMS

In Table I we tabulate the per-electron exchange energies $\epsilon_x = E_x/Z$ (in Ha/electron) for neutral atoms with $1 \leq Z \leq 120$. We include data for the spin-dependent local density approximation (LDA) and the optimized effective potential (OEP).

2. ENERGIES FOR POSITIVE IONS

Table II gives the data for selected positive ions, focusing on a series with the ratio of electron number to nuclear charge, N/Z , set to one-half. The beyond-LDA exchange energy per particle, $\Delta E_x/Z = (E_x - E_x^{\text{LDA}})/Z$, is included, and compared with the model suggested in the text: $-B(N/Z)\ln N - C$, with $B(N/Z)$ given by Eq. (18), and $-C$ equal to the beyond LDA value of the Hydrogen atom. The ratio $N/Z = 1/2$ probes a situation roughly halfway between the neutral atom and the Bohr atom, the two limits of Eq. (18) studied in detail. The $\ln Z$ term has been altered to $\ln N$ in order to produce reasonable results in the Bohr-atom limit and for single-electron systems (also included in the table). Replacing $\ln N$ by $\ln Z$ is equivalent to shifting C by $B\ln N/Z$, which is a constant for fixed N/Z . With the use of $\ln N$, the value of C used is 3% off from that for the Bohr atom (see the end of Sec. 4 below).

3. STATISTICAL FITS

In Table III we show systematic data fits for $\Delta E_x/Z = (E_x - E_x^{\text{LDA}})/Z$ for the neutral atoms of Table I. The first column indicates the data set used, as explained below, then coefficients with asymptotic standard errors from nonlinear regression, using the Levenberg-Marquardt method. Finally, the reduced χ^2 which is the χ^2 measure divided by the net

number of degrees of freedom in the fit. In calculating the reduced χ^2 , a standard error of 1 mHa is assumed for individual energy data points.

There are four data sets used here. “all” uses all atoms from $Z = 1$ to 120 indiscriminately. The large data set, “l”, consists of 16 data points, corresponding to atoms with closed s, p, d, and f shells, excluding the first occurrence of each series, He ($1s^2$), Ne ($2p^6$), Zn ($3d^{10}$) and Yb ($4f^{14}$). The atoms in the set thus consist of the filled 2s through 8s ($Z = 120$) alkali earths, 3p through 7p ($Z = 118$) noble gases, 4d through 6d group 12 transition metals and the filled 5f actinide. The net number of degrees of freedom varies from 12 to 15, depending on the number of fit parameters. The medium data set, labelled “m”, drops the next smallest closed shell of each series, the closed 2s, 3p, 4d and 5f shell atoms, and thus has 12 atoms. The “s” or small data set drops the next smallest shell (3s, 4p, 5d), for 9 atoms.

The basic model used for all fits is [Eq. (2) of main text]:

$$\Delta E_x(Z)/Z \approx -(A'Z^{1/3} + B \log Z + C + DZ^{-1/3})$$

which is fit versus $x = Z^{1/3}$, so the actual fit equation used is:

$$y = -A'x - 3B \log x - C - D/x.$$

Assuming $C \neq 0$, there are eight possible models formed by setting A , B or D to be either zero (in which case the data entry is left blank) or nonzero. All eight are shown here for completeness, but in the main text, the fifth, which is noncompetitive is omitted.

Z	LDA	OEP	Z	LDA	OEP	Z	LDA	OEP
1	-0.25643	-0.31250	41	-2.66072	-2.81060	81	-4.18152	-4.34816
2	-0.43087	-0.51288	42	-2.70355	-2.85462	82	-4.21322	-4.38052
3	-0.50477	-0.59358	43	-2.74045	-2.89248	83	-4.24477	-4.41280
4	-0.57258	-0.66644	44	-2.78341	-2.93574	84	-4.27513	-4.44358
5	-0.64936	-0.74854	45	-2.82457	-2.97753	85	-4.30552	-4.47437
6	-0.73837	-0.84105	46	-2.86983	-3.02421	86	-4.33591	-4.50526
7	-0.83672	-0.94349	47	-2.90896	-3.06390	87	-4.36394	-4.53342
8	-0.91253	-1.02256	48	-2.94660	-3.10166	88	-4.39146	-4.56096
9	-0.99989	-1.11145	49	-2.98276	-3.13854	89	-4.41983	-4.58942
10	-1.09667	-1.21050	50	-3.01882	-3.17524	90	-4.44834	-4.61803
11	-1.15723	-1.27391	51	-3.05481	-3.21198	91	-4.48309	-4.65237
12	-1.21362	-1.33236	52	-3.08888	-3.24639	92	-4.51534	-4.68464
13	-1.26815	-1.38945	53	-3.12318	-3.28100	93	-4.54795	-4.71740
14	-1.32461	-1.44808	54	-3.15765	-3.31599	94	-4.58464	-4.75454
15	-1.38288	-1.50894	55	-3.18824	-3.34653	95	-4.61813	-4.78864
16	-1.43435	-1.56220	56	-3.21811	-3.37619	96	-4.64777	-4.81868
17	-1.48856	-1.61782	57	-3.24965	-3.40767	97	-4.68219	-4.85217
18	-1.54512	-1.67637	58	-3.29489	-3.45176	98	-4.71470	-4.88459
19	-1.58748	-1.71931	59	-3.33473	-3.49126	99	-4.74752	-4.91745
20	-1.62795	-1.75995	60	-3.37534	-3.53175	100	-4.78064	-4.95077
21	-1.67794	-1.81033	61	-3.41663	-3.57320	101	-4.81404	-4.98456
22	-1.73095	-1.86381	62	-3.45858	-3.61558	102	-4.84774	-5.01882
23	-1.79706	-1.92995	63	-3.50114	-3.65889	103	-4.87607	-5.04771
24	-1.85542	-1.98981	64	-3.53680	-3.69514	104	-4.90703	-5.07926
25	-1.90284	-2.03933	65	-3.58066	-3.73645	105	-4.93670	-5.10953
26	-1.95511	-2.09125	66	-3.62133	-3.77647	106	-4.96638	-5.13987
27	-2.01567	-2.15052	67	-3.66260	-3.81731	107	-4.99609	-5.17034
28	-2.07288	-2.20820	68	nan	-3.87481	108	-5.02461	-5.19913
29	-2.13180	-2.26810	69	-3.74685	-3.90154	109	-5.05324	-5.22806
30	-2.18308	-2.32063	70	-3.78980	-3.94495	110	-5.08197	-5.25715
31	-2.23125	-2.37083	71	-3.82682	-3.98320	111	-5.11078	-5.28643
32	-2.27892	-2.42026	72	-3.86369	-4.02129	112	-5.13969	-5.31593
33	-2.32634	-2.46958	73	-3.90045	-4.05929	113	-5.16617	-5.34266
34	-2.37021	-2.51475	74	-3.93716	-4.09730	114	-5.19258	-5.36928
35	-2.41456	-2.56025	75	-3.97388	-4.13544	115	-5.21892	-5.39588
36	-2.45932	-2.60647	76	-4.00870	-4.17097	116	-5.24447	-5.42149
37	-2.49740	-2.64514	77	-4.04369	-4.20670	117	-5.27005	-5.44711
38	-2.53421	-2.68227	78	-4.08121	-4.24554	118	-5.29563	-5.47281
39	-2.57363	-2.72217	79	-4.11684	-4.28235	119	-5.31963	-5.49667
40	-2.61419	-2.76329	80	-4.14968	-4.31556	120	-5.34330	-5.52012

 TABLE I. Exchange energy per electron for neutral atoms for $Z = 1$ through $Z = 120$, using the PW92 local density approximation (LDA) and the optimized effective potential (OEP).

N	Z	OEP	LDA	$\Delta E_x/Z$	model	% difference
1	2	-0.3125	-0.2616	-0.0509	-0.0561	-10.2
2	4	-0.5693	-0.4829	-0.0864	-0.0766	11.4
4	8	-0.7443	-0.6461	-0.0982	-0.0971	1.1
10	20	-1.4872	-1.3591	-0.1280	-0.1241	3.0
12	24	-1.6026	-1.4736	-0.1290	-0.1295	-0.4
18	36	-2.0145	-1.8771	-0.1374	-0.1415	-3.0
1	1	-0.3125	-0.2564	-0.0561	-0.0561	-0.0
1	2	-0.3125	-0.2616	-0.0509	-0.0561	-10.2
1	4	-0.3125	-0.2646	-0.0479	-0.0561	-17.2
1	10	-0.3125	-0.2666	-0.0459	-0.0561	-22.3
1	12	-0.3125	-0.2669	-0.0456	-0.0561	-22.9
1	18	-0.3125	-0.2672	-0.0453	-0.0561	-24.0

 TABLE II. Exchange energies divided by Z for various positive ions. Shown are exact exchange using the OEP method, the LDA, the beyond-LDA contribution as compared to an asymptotic model, and the percent error of the model.

data set	A'	B	C	D	χ_{red}^2
all			0.1516(21)		530
l			0.153(6)		560
m			0.158(5)		359
s			0.163(5)		240
all			0.2048(16)	-0.179(5)	41.7
l			0.2138(34)	-0.205(11)	22.1
m			0.2269(25)	-0.256(9)	4.8
s			0.2328(24)	-0.279(9)	2.1
all		0.02432(24)	0.0589(9)		5.8
l		0.02464(26)	0.0590(10)		0.91
m		0.02538(26)	0.0560(11)		0.40
s		0.02535(32)	0.0562(13)		0.29
all		0.0260(9)	0.049(6)	0.013(7)	5.7
l		0.0256(14)	0.053(9)	0.008(12)	0.95
m		0.0238(23)	0.0667(16)	-0.016(23)	0.42
s		0.0225(35)	0.076(24)	-0.03(4)	0.30
all	0.0238(5)		0.0630(17)		21.
l	0.0230(10)		0.067(4)		16.
m	0.021(8)		0.0747(33)		5.8
s	0.0199(8)		0.0807(34)		3.0
all	0.0149(5)		0.1189(30)	-0.0759(39)	5.1
l	0.0128(9)		0.134(5)	-0.098(7)	1.3
m	0.0103(10)		0.154(7)	-0.136(12)	0.43
s	0.0090(14)		0.165(11)	-0.155(20)	0.33
all	0.0032(11)	0.0212(12)	0.0590(9)		5.5
l	0.0007(15)	0.0239(16)	0.0592(11)		0.96
m	-0.0013(20)	0.0285(35)	0.0549(20)		0.42
s	-0.0025(28)	0.0269(24)	0.0533(36)		0.30
all	0.014(4)	0.008(7)	0.117(19)	-0.073(24)	5.1
l	-0.007(8)	0.039(16)	0.01(5)	0.06(7)	0.98
m	0.003(17)	0.02(4)	0.09(15)	-0.05(20)	0.47
s	-0.025(35)	0.08(8)	-0.16(34)	0.3(5)	0.33

TABLE III. Coefficients and statistics for data fits to neutral atoms. Coefficients match those of Eq. (2) and Table I of the main text.

4. THE BOHR ATOM

The exchange energies for the Bohr atom were fit by defining a residual

$$R_o(N) = [E_x^{\text{Bohr}}(N) + \bar{A}_o N^{5/3}] / N,$$

in lieu of $E_x^{\text{Bohr}}(N)$ itself (recall that $\bar{A}_o = (2/3)^{1/3}(4/\pi^2)$). The values of this residual are provided in Table IV for up to $n = 22$ full shells, and are seen to vary nearly linearly in $\ln N$, with the deviations from linearity decreasing for large N . In order to obtain many-digit accuracy for the coefficients, a second residual,

$$S_o(N) = [R_o(N) + \bar{B}_o \ln N + \bar{C}_o] N^{2/3},$$

was defined, and it too varies nearly linearly in $\ln N$. The most accurate fit was obtained by inspecting visually plots of $S_o(N) + \bar{D}_o \ln N$ vs. $\ln N$, magnifying the deviation of the second residual from linearity in $\ln N$, and adjusting the values of the coefficients so that the deviations from linearity at large N are minimal [once it was guessed that $\bar{B}_o = 7/(27\pi^2)$, the analytic value was used for subsequent refinement, so that no more than two coefficients needed to be simultaneously adjusted]. Obtaining smooth plots requires retaining more than 6 significant digits in $R_o(N)$, due to the multiplication by $N^{2/3}$ and the magnification (even more significant digits are required in $E_x^{\text{Bohr}}(N)$, of course).

For the LDA applied to the Bohr atom, a residual $R_o^{\text{LDA}}(N)$ was similarly defined, with values given in Table V. In this case the deviations from linearity are greater,

due to the presence of additional terms in the expansion — here, the second residual would be defined with a power of $N^{1/3}$ rather than $N^{2/3}$. The similarity of the $\propto N$ and the $\propto N^{2/3} \ln N$ behaviors over a large range of N makes fitting by visual inspection difficult (the accuracy achieved for \bar{B}_o^{LDA} based on data up to $n = 28$ shells was circa 1%, leaving some room for questions regarding the use of the analytic value). Luckily, extension of the data set to very large values of N is accessible, up to $n = 100$ shells here, and an automated fit provides sufficient accuracy (which is gauged by comparison to fits with more limited ranges of data).

The fit gives $\bar{B}_o^{\text{LDA}} = -7.505$ mHa and $\bar{C}_o^{\text{LDA}} = -9.2$ mHa (further coefficients were not carefully extracted). Extracting the beyond-LDA coefficient as in Eq. (12) gives $C_o = 54.6$ mHa for the Bohr atom, which differs by only a few percent from the neutral-atom value in Eq. (3).

n	N	$R_o(N)$
1	2	-0.06298252
2	10	-0.10453258
3	28	-0.13185039
4	60	-0.15211566
5	110	-0.16821274
6	182	-0.18156344
7	280	-0.19296926
8	408	-0.20292569
9	570	-0.21176023
10	770	-0.21970057
11	1012	-0.22691143
12	1300	-0.23351580
13	1638	-0.23960797
14	2030	-0.24526180
15	2480	-0.25053622
16	2992	-0.25547902
17	3570	-0.26012950
18	4218	-0.26452035
19	4940	-0.26867906
20	5740	-0.27262896
21	6622	-0.27639005
22	7590	-0.27997958

TABLE IV. The residual of the exchange energy per electron for Bohr atoms with n complete shells. N is the number of electrons.

n	N	$R_o^{\text{LDA}}(N)$	n	N	$R_o^{\text{LDA}}(N)$	n	N	$R_o^{\text{LDA}}(N)$	n	N	$R_o^{\text{LDA}}(N)$
1	2	0.02594248	26	12402	0.08262241	51	91052	0.09663426	76	298452	0.10511544
2	10	0.03499465	27	13860	0.08339534	52	96460	0.09704426	77	310310	0.10539532
3	28	0.04156255	28	15428	0.08414161	53	102078	0.09744674	78	322478	0.10567170
4	60	0.04657061	29	17110	0.08486301	54	107910	0.09784198	79	334960	0.10594467
5	110	0.05059082	30	18910	0.08556118	55	113960	0.09823025	80	347760	0.10621431
6	182	0.05394465	31	20832	0.08623759	56	120232	0.09861179	81	360882	0.10648071
7	280	0.05682234	32	22880	0.08689356	57	126730	0.09898682	82	374330	0.10674393
8	408	0.05934382	33	25058	0.08753032	58	133458	0.09935556	83	388108	0.10700407
9	570	0.06158899	34	27370	0.08814897	59	140420	0.09971824	84	402220	0.10726118
10	770	0.06361357	35	29820	0.08875052	60	147620	0.10007504	85	416670	0.10751533
11	1012	0.06545792	36	32412	0.08933592	61	155062	0.10042615	86	431462	0.10776661
12	1300	0.06715218	37	35150	0.08990601	62	162750	0.10077175	87	446600	0.10801506
13	1638	0.06871947	38	38038	0.09046158	63	170688	0.10111202	88	462088	0.10826076
14	2030	0.07017791	39	41080	0.09100336	64	178880	0.10144712	89	477930	0.10850376
15	2480	0.07154194	40	44280	0.09153204	65	187330	0.10177720	90	494130	0.10874413
16	2992	0.07282331	41	47642	0.09204822	66	196042	0.10210242	91	510692	0.10898191
17	3570	0.07403166	42	51170	0.09255251	67	205020	0.10242291	92	527620	0.10921717
18	4218	0.07517502	43	54868	0.09304543	68	214268	0.10273881	93	544918	0.10944996
19	4940	0.07626018	44	58740	0.09352751	69	223790	0.10305025	94	562590	0.10968033
20	5740	0.07729287	45	62790	0.09399920	70	233590	0.10335737	95	580640	0.10990833
21	6622	0.07827803	46	67022	0.09446095	71	243672	0.10366027	96	599072	0.11013401
22	7590	0.07921992	47	71440	0.09491317	72	254040	0.10395907	97	617890	0.11035741
23	8648	0.08012225	48	76048	0.09535626	73	264698	0.10425388	98	637098	0.11057859
24	9800	0.08098825	49	80850	0.09579058	74	275650	0.10454481	99	656700	0.11079758
25	11050	0.08182080	50	85850	0.09621647	75	286900	0.10483197	100	676700	0.11101443

TABLE V. The residual for the Bohr atom within the LDA.